Heliyon 10 (2024) e22772

Contents lists available at ScienceDirect

Heliyon

journal homepage: www.cell.com/heliyon

MiR-2113 overexpression attenuates sepsis-induced acute pulmonary dysfunction, inflammation and fibrosis by inhibition of HMGB1

Yong Li [a], Hui-Ling Xu [a], Xiu-Wen Kang [a], Suo Xu [b], Zhi-Fang Mou [a,*]

[a] Department of Critical Care Medicine, The First People's Hospital of Lianyungang, Lianyungang, Jiangsu, China
[b] Department of Emergency Medicine, The First People's Hospital of Lianyungang, Lianyungang, Jiangsu, China

ARTICLE INFO

Keywords:
MiR-2113
Sepsis
Acute pulmonary dysfunction
Inflammation
fibrosis
High-mobility group box 1

ABSTRACT

Purpose: Sepsis-induced acute lung injury is related to high mortality. MiR-2113 possesses important functions in human diseases. This research aimed to clarify the role and mechanism of miR-2113 in sepsis-induced acute lung injury.

Methods: The expression of miR-2113 in lipopolysaccharide (LPS)-induced MLE-12 cells, serum of sepsis patients, and cecal ligation and puncture mouse models was examined using quantitative real-time PCR. The functions of miR-2113 in LPS-treated MLE-12 cells were estimated by Cell Counting Kit-8 assay, flow cytometry, enzyme-linked immunosorbent assay, Western blot, and immunofluorescence. The influences of miR-2113 in cecal ligation and puncture-induced acute lung injury in mice were assessed by hematoxylin-eosin staining, terminal deoxynucleotidyl transferase-mediated dUTP-biotin nick end labeling assay, acute pulmonary dysfunction analysis, lactate dehydrogenase levels and total protein concentrations in bronchoalveolar lavage fluid, and Masson staining. Also, the mechanism of miR-2113 was examined using a dual-luciferase reporter assay.

Results: MiR-2113 expression was decreased in LPS-induced MLE-12 cells, serum of sepsis patients, and cecal ligation and puncture mouse models. miR-2113 overexpression restored LPS-reduced MLE-12 cell proliferation, but alleviated LPS-induced apoptosis and markers of inflammation and fibrosis in MLE-12 cells. Moreover, we found that miR-2113 mimic reduced LPS-induced MLE-12 cell injury by negatively regulating high-mobility group box 1. *In vivo* data further confirmed that miR-2113 overexpression alleviated acute pulmonary dysfunction, inflammation and fibrosis in cecal ligation and puncture-induced sepsis mice.

Conclusion: MiR-2113 relieved sepsis-induced acute pulmonary dysfunction, inflammation and fibrosis through decreasing high-mobility group box 1.

1. Introduction

Sepsis is a condition of physiological, pathological, and biochemical abnormalities induced by the host's uncontrolled response to infection, and multi-organ dysfunction is the primary cause of death [1,2]. The lung is the first organ to respond to sepsis, and sepsis

* Corresponding author. Department of Critical Care Medicine, The First People's Hospital of Lianyungang, No. 6, Zhenhua Road, Haizhou District, Lianyungang, Jiangsu 222000, China.
E-mail address: mouzhifanglyg@21cn.com (Z.-F. Mou).

https://doi.org/10.1016/j.heliyon.2023.e22772
Received 17 March 2023; Received in revised form 13 October 2023; Accepted 19 November 2023
Available online 23 November 2023

can cause acute lung injury (ALI) [3]. The progression of sepsis-induced ALI is usually accompanied by increases of inflammation and fibrosis [4,5]. Hence, searching for strategies to reduce inflammation and fibrosis might offer novel opportunities to ameliorate sepsis-induced ALI in humans.

MicroRNAs (miRNAs) modulate gene expression at the post-transcriptional level by decreasing messenger RNAs (mRNAs) levels to mediate cell proliferation, differentiation and other biological processes [6]. Recent studies have found that miRNAs are implicated in regulating the process of sepsis-induced ALI. For instance, miR-326 agomir prevented the inflammation and oxidative stress in cell and mouse models of sepsis-induced ALI by decreasing Toll-like receptors [7]. Also, miR-145 expression was decreased in lipopolysaccharide (LPS)-treated BEAS-2B cells, and miR-145 suppressed LPS-induced inflammation and sepsis-induced ALI [8]. Nevertheless, the miRNAs relevant to sepsis-induced ALI have not been fully elucidated.

MiR-2113 is located at chromosome 6q16.1 [9], and is a newly identified miRNA that has vital regulatory functions in numerous human diseases. For example, inhibition of miR-2113 decreased high-glucose-induced mesenchymal cell activation and fibrosis through RP11-982M15.8/Zeb1 [9]. Upregulation of miR-2113 reduced hepatocellular carcinoma cell proliferation and epithelial-mesenchymal transition [10]. However, the function of miR-2113 in sepsis-induced ALI has not been reported.

In the current research, we found that miR-2113 expression was decreased in LPS-induced MLE-12 cells and cecal ligation and puncture (CLP) mouse models as well as the serum of sepsis patients. The gain-of-function assay demonstrated that miR-2113 overexpression mitigated the inhibition of cell proliferation and reduced inflammatory and fibrosis markers in MLE-12 cells caused by LPS. Moreover, miR-2113 upregulation decreased acute pulmonary dysfunction, lung inflammation and fibrosis in CLP-treated mice. Additionally, this study further revealed the mechanism of miR-2113 in sepsis-induced ALI, aiming to supply effective therapeutic targets for sepsis-induced ALI.

2. Materials and methods

2.1. Clinical samples

Serum of sepsis patients (n = 32, 53.6 ± 6.1 years old) and healthy subjects (n = 25, 46.7 ± 5.8 years old) were obtained from The First People's Hospital of Lianyungang.

2.2. Cell culture and treatment

Mouse lung epithelial (MLE)-12 cells were provided by HyCyte (Suzhou, China) and were grown in F12/DMEM (SH30023.01, BasalMedia, Shanghai, China) with 10 % fetal bovine serum (FBS; 10099141C, Gibco, New York, USA). Cells were cultured at 37 °C and 5 % CO_2. MLE-12 cells were exposed to 0, 1, 2.5, 5, and 10 μg/ml LPS (CS0158, G-CLONE, Beijing, China) for 24 h [11,12].

2.3. Cell transfection

MiR-2113 mimic, miR-NC (a negative control for miR-2113 mimic), pcDNA-high-mobility group box 1 (HMGB1), and relevant controls were obtained from GenePharma (Shanghai, China).

MLE-12 cells (5×10^3) were grown in 96-well plates overnight. MiR-2113 mimic (100 pmol) and pcDNA-HMGB1 (50 nM) were transfected into MLE-12 cells using Lipofectamine 3000 (L3000-015, Invitrogen, Waltham, USA) when the cells reached 80 % confluency. The ratio of DNA and Lipofectamine 3000 was 1:1 [13]. The transfection lasted for 48 h before LPS treatment.

2.4. Construction of sepsis mouse model

C57BL/6 mice (6–8 weeks old) were from Gempharmatech (Nanjing, China). Mice were maintained in a 12 h light/dark cycle with 22–24 °C. Animal protocol was approved by Ethical Review Committee of The First People's Hospital of Lianyungang (KY-20220226001-02) and was actualized following the ARRIVE guidelines (https://arriveguidelines.org).

Agomir-NC and agomir-miR-2113 were provided by Ribobio (Guangzhou, China). Mice were divided into sham, CLP, CLP + agomir-NC and CLP + agomir-miR-2113 groups (n = 6 per group). After fasting for 12 h, all mice were anesthetized by intraperitoneal injection of 1 % pentobarbital sodium (80 μg/g body weight, #11715, Sigma-Aldrich, Missouri, USA). For the CLP group, mice were anesthetized and a 1 cm incision was made along the midline of the abdomen. The cecum was exposed, ligated and pierced. Then, the cecum was returned to the peritoneal cavity and the peritoneum was closed. For mice in the sham group, the cecum was exposed without ligation or puncture. For mice in the CLP + agomir-NC and CLP + agomir-miR-2113 groups, 30 mg/kg agomir-NC or agomir-miR-2113 was injected through a tail vein [14]. After one day, mice were sacrificed by intraperitoneal injection of phenobarbital (200 mg/kg) [15]. The trachea of mouse was exposed, and the lung was infused with three aliquots of phosphate buffer solution (PBS) (0.3, 0.3, 0.4 ml) through trachea. Afterward, the bronchoalveolar lavage fluid (BALF) was collected, centrifuged (400×*g*, 3 min) at 4 °C, and then kept at −80 °C.

2.5. Quantitative real-time PCR (qRT-PCR)

Total RNAs were extracted with Trizol (abs60154, Absin, Shanghai, China). The cDNAs were obtained using MicroRNA Reverse Transcription Kits (EZB-miRT3/EZB-miRT3-L, EZBioscience, California, USA) or PrimeScriptTM RT Master Mix (RR036A, TaKaRa,

Beijing, China). qRT-PCR was conducted to determine the expressions of mRNAs and miRNAs on the LightCycler480 Real-Time PCR System (Roche, Switzerland) using SYBR Green mix (RR820A, TaKaRa). Procedures were 95 °C for 2 min; 40 cycles of 95 °C for 10 s, 60 °C for 15 s, and 72 °C for 25 s. The expressions of mRNAs and miRNAs were calculated with the $2^{-\Delta\Delta CT}$ method after normalizing to the values of GAPDH and U6, respectively. Primer sequences are displayed in Table 1.

2.6. Cell Counting Kit-8 assay

MLE-12 cells (4×10^3) were grown in 96-well plates. After culturing for 24 h, cells were exposed to 10 μl Cell Counting Kit-8 (abs50003, CCK-8, Absin) reagent for 1.5 h. Absorbance (450 nm) was tested using a microplate spectrophotometer (Cisbio, Shanghai, China).

2.7. Flow cytometry

MLE-12 cells were collected and washed with PBS. Then, cell density was adjusted to 2×10^6 cells/ml by resuspending in 1 × Annexin V binding buffer (P-CA-151, Procell, Wuhan, China). Subsequently, MLE-12 cells were stained with Annexin V-FITC/PI Cell Apoptosis Detection Kits (P-CA-201, Procell) according to the manufacturer's protocol. The apoptosis of MLE-12 cells was analyzed by a flow cytometer (Nanofcm, Xiamen, China) combined with CellQuest software (version 3.0, Becton Dickinson, New York, USA).

2.8. Enzyme-linked immunosorbent assay (ELISA)

The levels of proinflammatory cytokines (interleukin (IL)-1β, IL-6 and tumor necrosis factor (TNF)-α) in MLE-12 cells and mouse BALF were examined using corresponding commercial ELISA kits (E-EL-M0037c, E-EL-M0044c, E-EL-M3063; Elabscience, Wuhan, China). Absorbance was measured at 450 nm within 25 min of the reaction using a microplate reader (DNM-9606, PERLONG, Beijing, China).

2.9. Western blot

Total proteins were extracted using RIPA lysis buffer (P0013B, Beyotime, Shanghai, China). Subsequently, proteins were quantified using BCA Kits (P0009, Beyotime) and separated with 12 % SDS-PAGE (M01215C, Genscript, Nanjing, China). Proteins were transferred onto PVDF membranes (1620177, Bio-Rad, California, USA). Then, membranes were blocked and exposed to primary antibodies against alpha-smooth muscle actin (α-SMA, ab124964, 1/10000), fibronectin (FN, ab2413, 1/1000), collagen I (ab138492, 1/2000), HMGB1 (ab18256, 1 μg/ml), IL-1β (ab254360, 1/1000), IL-6 (ab233706, 1/1000), TNF-α (ab183218, 1/2000), and β-actin (ab8226, 1 μg/ml) overnight, followed by incubation with secondary antibodies (ab205718, 1/2000). All antibodies were provided by Abcam (Cambridge, UK). Protein bands were visualized using ECL Kits (ml095429, Mlbio, Shanghai, China). Density of protein bands was examined with Alphalmager™ 2000 Imaging System (Alpha Innotech, USA).

2.10. Immunofluorescence assay

MLE-12 cells were fixed with 4 % paraformaldehyde (PN4204, G-CLONE) and exposed to BSA (ab245930, Abcam) for 25 min. Then, cells were incubated with antibodies against α-SMA (ab124964, 1/300, Abcam) overnight and FITC-labelled secondary antibody (ab7086, 1/2000, Abcam) for 1 h. Nuclei were dyed with DAPI (ab285390, Abcam), and images were obtained using a microscope (Olympus, Japan). α-SMA expression was quantified using Image J software (National Institutes of Health, Maryland, USA). The

Table 1
Primers sequences.

Gene name	Primer sequence (5′-3′)
MiR-2113	Forward: TGTGCTTGGCTCTGTCA
	Reverse: GAACATGTCTGCGTATCTC
α-SMA	Forward: CTGTTCCAGCCATCCTTCAT
	Reverse: TCATGATGCTGTTGTAGGTGGT
FN	Forward: GCCACTGGAGTCTTTACCACA
	Reverse: CCTCGGTGTTGTAAGGTGGA
Collagen I	Forward: GGGATTCCCTGGACCTAAAG
	Reverse: GGAACACCTCGCTCTCCA
HMGB1	Forward: GCCCATTTTGGGTCACATGG
	Reverse: TGCAGGGTGTGTGGACAAAA
GAPDH	Forward: GCTCTCTGCTCCTCCTGTTC
	Reverse: ACGACCAAATCCGTTGACTC
U6	Forward: CTCGCTTCGGCAGCACA
	Reverse: AACGCTTCACGAATTTGCGT

FN: Fibronectin.

formula used was as follows: Mean fluorescence intensity = Integrated Density/Area.

2.11. Dual-luciferase reporter assay

The binding sites between miR-2113 and HMGB1 were forecasted by TargetScan software (www.targetscan.org). Fragments with a predicted sequence of HMGB1-wild-type (WT), or HMGB1-mutant (MUT) were cloned into a pGL3 vector (Promega, USA).

MLE-12 cells (1×10^6) were grown in 6-well plates overnight. Afterward, the constructed pGL3-HMGB1-WT or pGL3-HMGB1-MUT vector was transfected into MLE-12 cells with miR-2113 mimic or miR-NC. 48 h later, the relative luciferase activity was examined. In brief, cell culture medium was removed and 100 μl PBS was added to wash the cells. Subsequently, 100 μl lysis solution was added and plates were shaken for 10–15 min to collect cell lysate. Then, cell lysate (25 μl) was mixed with 100 μl luciferase assay reagent. Reporter gene activity was expressed as the ratio of firefly luciferase activity to Renilla luciferase activity.

2.12. Hematoxylin-eosin staining

Mouse lung tissues were fixed with 4 % paraformaldehyde, and 4 μm continuous sections were prepared. Then, sections were dyed with hematoxylin (GH0030, G-CLONE) for 3 min. After washing, sections were exposed to Eosin (CS1703, G-CLONE) for 2 min. Pathological changes in mouse lung tissues were estimated with a light microscope.

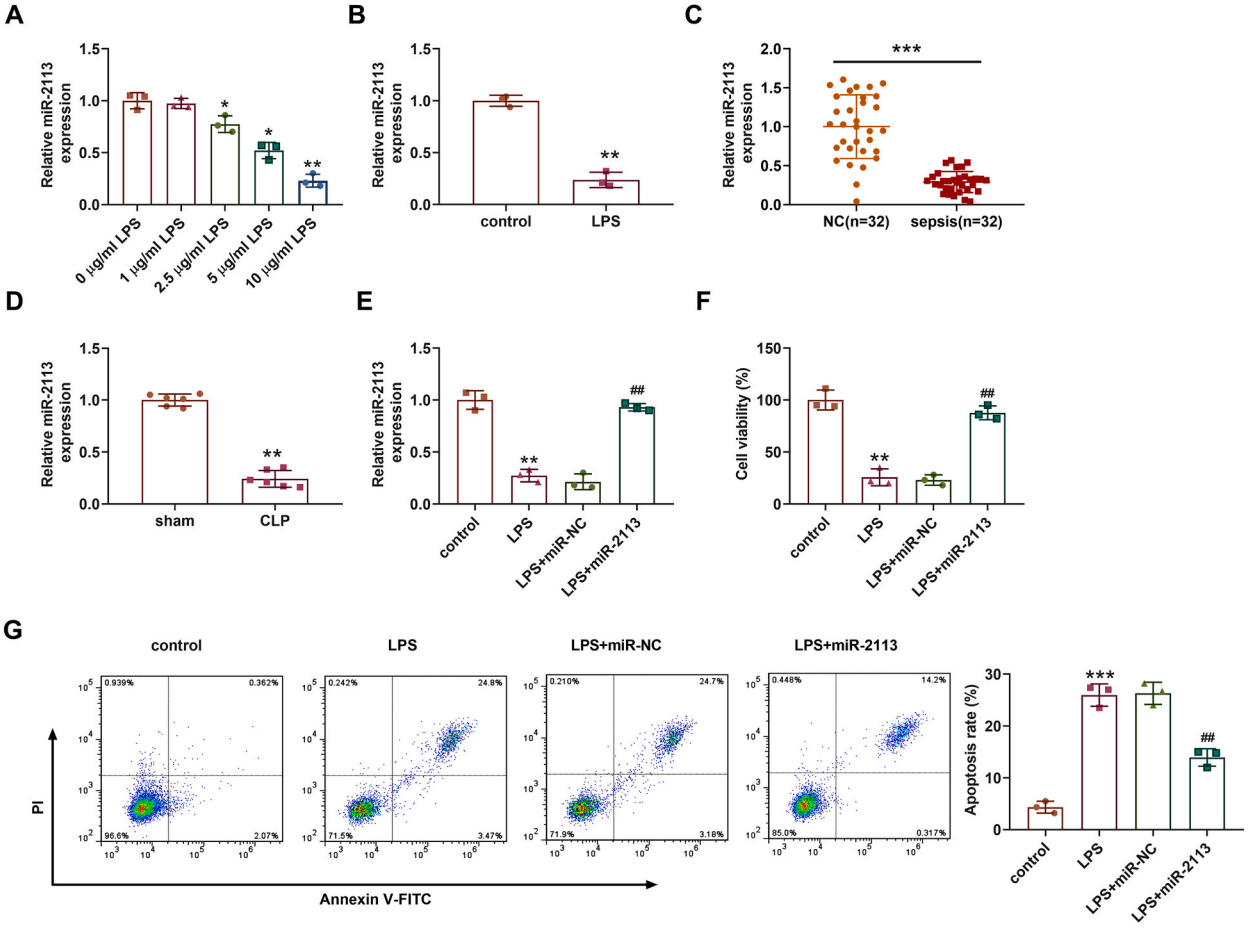

Fig. 1. Expressions of miR-2113 in LPS-induced MLE-12 and cecal ligation and puncture mouse models. (A) MLE-12 cells were exposed to 0, 1, 2.5, 5, or 10 μg/ml LPS for 24 h. MiR-2113 expression in LPS-induced MLE-12 cells was examined using qRT-PCR. (B) MLE-12 cells were exposed to 10 μg/ml LPS for 24 h and miR-2113 expression was tested by qRT-PCR. (C) Analysis of miR-2113 expression in the serum of sepsis patients (n = 32) and healthy subjects by qRT-PCR. (D) MiR-2113 expression in mouse lung tissues (n = 6) was measured by qRT-PCR. (E) MiR-2113 mimic was transfected into LPS-induced MLE-12 cells for 48 h miR-2113 expression was detected by qRT-PCR. (F) MLE-12 cell proliferation was checked using Cell Counting Kit-8 (CCK-8) assay. (G) MLE-12 cell apoptosis was determined via flow cytometry. $^{*}P < 0.05$ vs. control. $^{**}P < 0.01$ vs. control or sham. $^{***}P < 0.001$ vs. control. $^{\#\#}P < 0.01$ vs. LPS + miR-NC. Con: control. CLP: cecal ligation and puncture. LPS: lipopolysaccharide. miR-NC: miR-2113 negative control. Data are expressed as mean ± SD of at least three independent experiments. Differences were assessed with Student's *t*-test or one-way ANOVA followed by Tukey's post-test.

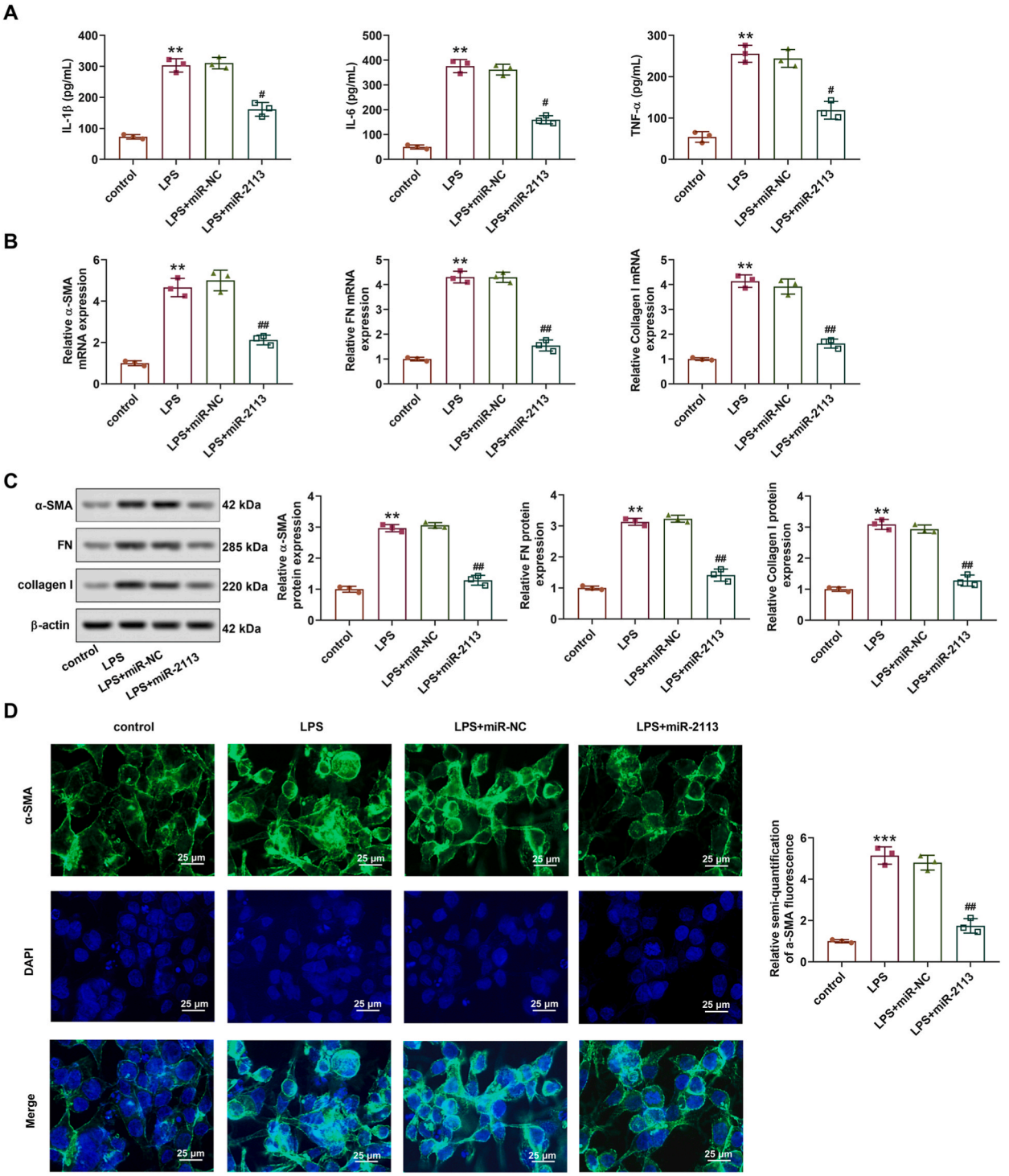

Fig. 2. MiR-2113 modulates inflammatory and fibrosis markers in LPS-induced MLE-12 cells. MiR-2113 mimic was transfected into LPS-induced MLE-12 cells for 48 h. (A) The levels of proinflammatory cytokines IL-1β, IL-6, and TNF-α were checked by ELISA. (B) The mRNA levels of fibrosis markers α-SMA, FN, and collagen I were detected using qRT-PCR. (C) The protein levels of α-SMA, FN, and collagen I in MLE-12 cells were tested via Western blot. (D) Detection of α-SMA expression with immunofluorescence assay, α-SMA (green), nuclei (blue) (scale bar: 25 μm). $^{**}P < 0.01$, $^{***}P < 0.001$ vs. control. $^{\#}P < 0.05$, $^{\#\#}P < 0.01$ vs. LPS + miR-NC. WT: wild-type. MUT: mutant. FN: fibronectin. Data are expressed as mean ± SD of at least three independent experiments. Differences were assessed with one-way ANOVA followed by Tukey's post-test. (For interpretation of the references to colour in this figure legend, the reader is referred to the Web version of this article.)

2.13. Terminal deoxynucleotidyl transferase-mediated dUTP-biotin nick end labeling (TUNEL) assay

After being de-waxed and dehydrated, tissues in the 4 μm sections were eliminated endogenous peroxidase activity. Thereafter, sections were exposed to TUNEL reagent (TUNEL Assay Kit, ab206386, Abcam) for 1.5 h. Then, sections were dyed with DAB solution (ab206386, Abcam) for 10 min. Lastly, sections were observed under a microscope.

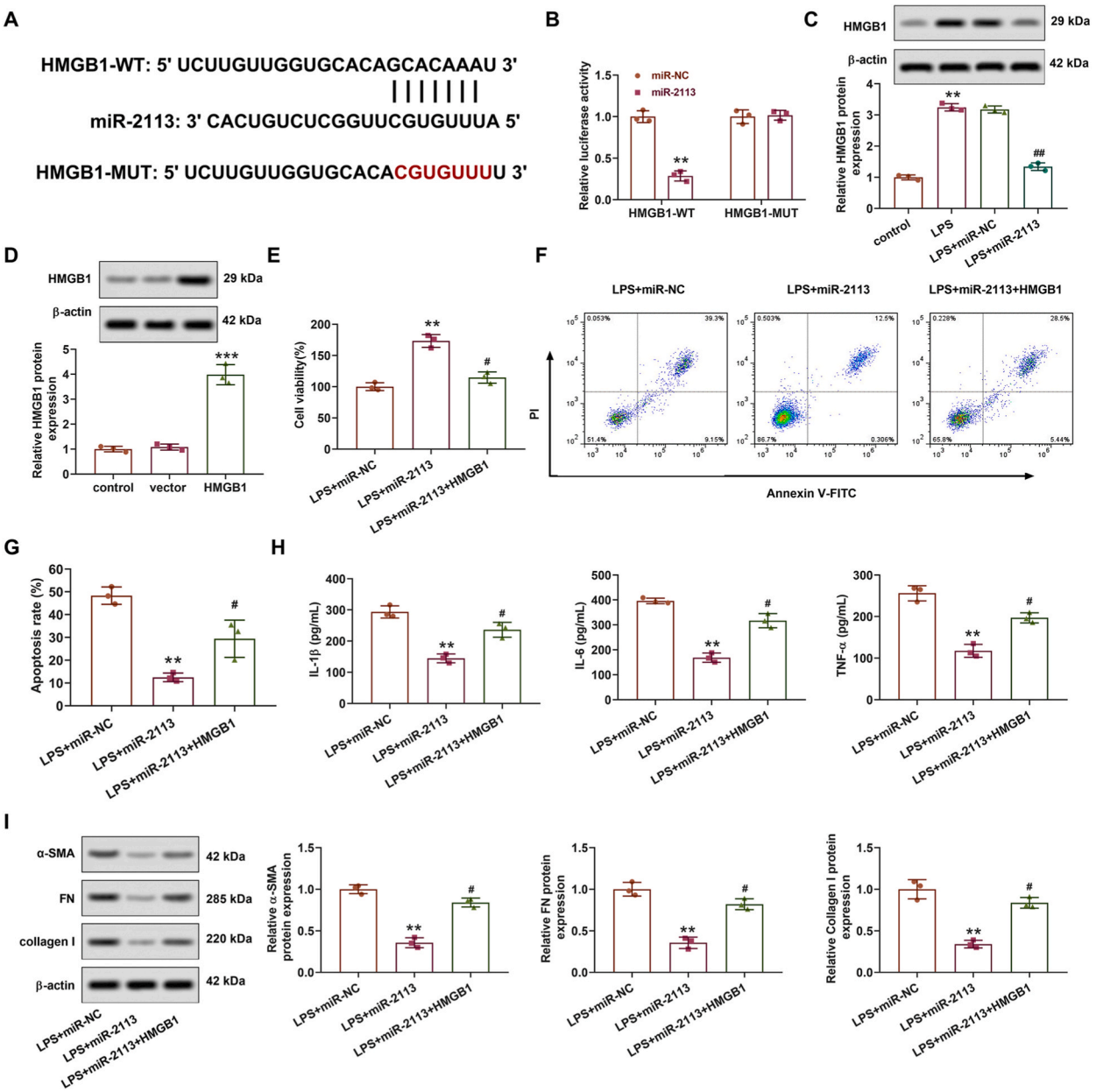

Fig. 3. MiR-2113 modulates LPS-induced MLE-12 cell injury through high mobility group protein 1. (A) MiR-2113 targeting HMGB1 was predicted by Targetscan. (B) Validation of miR-2113 targeting HMGB1 using a dual-luciferase reporter assay. (C) MiR-2113 mimic was transfected into LPS-induced MLE-12 cells for 48 h. Determination of HMGB1 protein levels by Western blot. (D) pcDNA-HMGB1 was transfected into MLE-12 cells for 48 h. Western blot analysis of HMGB1 protein levels. (E) MiR-2113 mimic and/or pcDNA-HMGB1 were transfected into LPS-induced MLE-12 cells for 48 h. MLE-12 cell proliferation was checked with CCK-8 assay. (F–G) Flow cytometry analysis of MLE-12 cell apoptosis. (H) The contents of IL-1β, IL-6, and TNF-α were tested using ELISA. (I) Western blot was used to determine the protein levels of α-SMA, FN, and collagen I. $^{**}P < 0.01$ vs. miR-NC, control, or LPS + miR-NC. $^{***}P < 0.001$ vs. vector. $^{\#}P < 0.05$, $^{\#\#}P < 0.01$ vs. LPS + miR-2113 mimic. HMGB1: high mobility group protein 1. Data are expressed as mean ± SD of at least three independent experiments. Differences were assessed by Student's *t*-test or one-way ANOVA followed by Tukey's post-test.

2.14. Analysis of acute pulmonary dysfunction in mice

Mouse lung function was estimated using the Buxco pulmonary function testing system (Connecticut, USA) following a previously reported method [16]. Airway resistance, lung ventilation, lung compliance, tidal volume, and respiratory rate (RR) were recorded from a FluxMed monitor (MBMed, Buenos Aires, Argentina) in anesthetized mice following the reported methods [17,18].

The wet/dry (W/D) ratio of mouse lung tissues was checked [19]. Fresh lung tissues were weighed to obtain the wet weight. The lung tissues were then dried at 80 °C and the weight was measured again.

2.15. Lactate dehydrogenase (LDH) levels and total protein concentrations in BALF

LDH levels were estimated using LDH Activity Assay Kits (E-BC-K046-M, Elabscience) as manufacturer's procedures.

After centrifugation at 1600 rpm for 8 min, the supernatant of BALF was gathered. Total protein contents in BALF were determined by BCA Kits (P0009, Beyotime).

2.16. Masson staining

The degree of pulmonary fibrosis in mice was evaluated using Masson staining. The 4 μm sections were prepared and dyed with celestine blue dye solution (BP-DL008, Sbjbio, Nanjing, China) for 3 min, followed by dyeing with hematoxylin (GH0030, G-CLONE) and Lichun red acid (RS1850, G-CLONE) for 5 min. Then, the sections were stained with 1 % phosphomolybdic acid (RS2780, G-CLONE) and examined with a microscope.

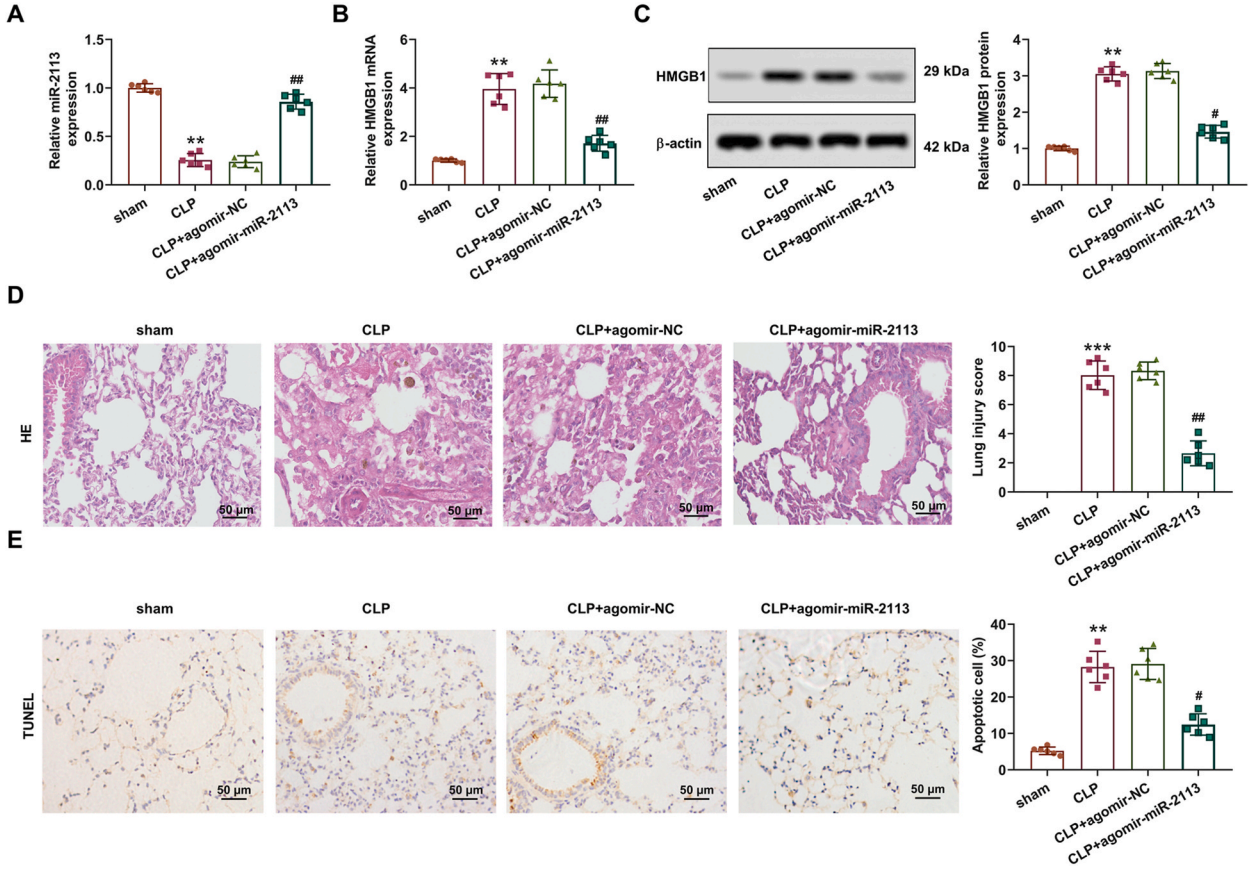

Fig. 4. MiR-2113 overexpression relieves lung injury in mice induced by sepsis. 30 mg/kg agomir-NC or agomir-miR-2113 was injected into the CLP-induced sepsis mouse model through a tail vein. Mice were grouped into the sham, CLP, CLP + agomir-NC and CLP + agomir-miR-2113 groups (n = 6 per group). (A) MiR-2113 expression was measured by qRT-PCR. (B–C) HMGB1 mRNA and protein levels in mouse lung tissues were checked using qRT-PCR and Western blot. (D) Pathological changes in mouse lung tissues were identified by hematoxylin-eosin staining (scale bar: 100 μm). (E) The apoptosis of mouse lung tissues was evaluated with TUNEL analysis (scale bar: 200 μm). $^{**}P < 0.01$, $^{***}P < 0.001$ vs. sham. $^{\#}P < 0.05$, $^{\#\#}P < 0.01$ vs. CLP + agomir-NC. CLP: cecal ligation and puncture. HE: hematoxylin-eosin. Differences were assessed with one-way ANOVA followed by Tukey's post-test.

2.17. Statistical analysis

Statistical analyses were performed with SPSS software (Chicago, USA). Data were exhibited as mean ± standard deviation (SD). Differences between two groups were compared using Student's *t*-test, and the differences among three or more groups were evaluated using one-way ANOVA followed by Tukey's post-test. Statistical significance was defined when $P < 0.05$.

3. Results

3.1. MiR-2113 expression in LPS-induced MLE-12 cells and CLP mouse models

To illuminate the function of miR-2113 in sepsis, miR-2113 expression in sepsis models was firstly examined. MLE-12 cells were treated with different concentrations (0, 1, 2.5, 5, and 10 μg/ml) of LPS. The results showed that the expression of miR-2113 in MLE-12 cells was decreased by LPS, with the lowest in 10 μg/ml LPS. Hence, 10 μg/ml LPS was applied in this research (Fig. 1A). As seen in Fig. 1B–D, miR-2113 was under-expressed in LPS-induced MLE-12 cells, serum of sepsis patients, and CLP mouse models. Then, miR-2113 mimic was transfected into LPS-induced MLE-12 cells to explore the role of miR-2113 in sepsis *in vitro* (Fig. 1E). miR-2113 mimic enhanced the proliferation of MLE-12 cells that was decreased by LPS (Fig. 1F). Also, miR-2113 mimic reduced LPS-induced apoptosis in MLE-12 cells (Fig. 1G). These data elucidated that miR-2113 overexpression mitigated LPS-mediated inhibition of proliferation in MLE-12 cells.

3.2. MiR-2113 mimic alleviates inflammatory and fibrosis markers in LPS-induced MLE-12 cells

LPS-induced proinflammatory cytokines (IL-1β, IL-6, and TNF-α) in MLE-12 cells was abolished by miR-2113 mimic (Fig. 2A). Meanwhile, miR-2113 mimic suppressed the mRNA and protein levels of fibrosis markers (α-SMA, FN, and collagen I) induced by LPS in MLE-12 cells (Fig. 2B and C, Supplementary File-2). Immunofluorescence results further elucidated that the α-SMA levels were increased by LPS, the effect of which was decreased by miR-2113 mimic (Fig. 2D). These results suggested that miR-2113 overexpression reduced inflammatory and fibrosis markers in LPS-stimulated MLE-12 cells.

3.3. MiR-2113 modulates LPS-induced MLE-12 cell injury through targeting HMGB1

To clarify the downstream mechanism of miR-2113, Targetscan software was used to predict the target genes of miR-2113 and we found that HMGB1 was a target of miR-2113 (Fig. 3A). We further verified that miR-2113 mimic reduced the luciferase activity of HMGB1-WT, but had no obvious impact on HMGB1-MUT (Fig. 3B). The protein levels of HMGB1 induced by LPS was decreased by

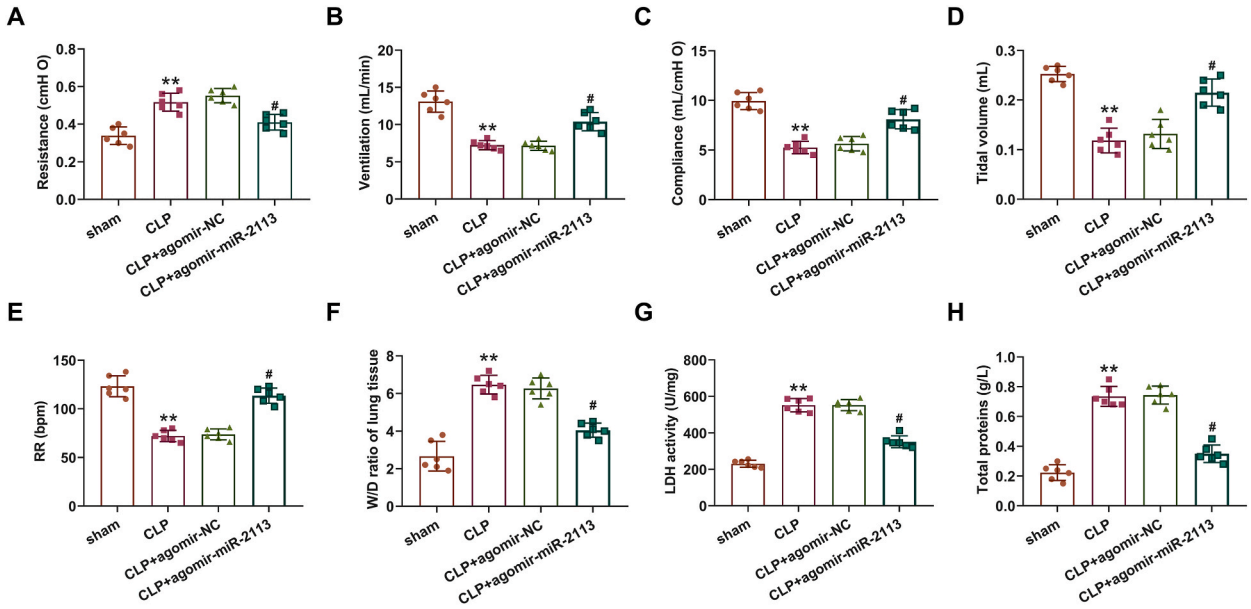

Fig. 5. MiR-2113 influences acute pulmonary dysfunction in mice induced by sepsis. Mice were grouped into the sham, CLP, CLP + agomir-NC and CLP + agomir-miR-2113 groups (n = 6 per group). Detection of airway resistance (A), lung ventilation (B), lung compliance (C), tidal volume (D), and respiratory rate (RR) (E). (F) Wet/dry (W/D) ratio. LDH levels (G) and total protein concentrations (H) in BALF. $^{**}P < 0.01$ vs. sham. $^{\#}P < 0.05$ vs. CLP + agomir-NC. RR: respiratory rate. W/D: Wet/dry. LDH: lactate dehydrogenase. BALF: bronchoalveolar lavage fluid. Differences were assessed with one-way ANOVA followed by Tukey's post-test.

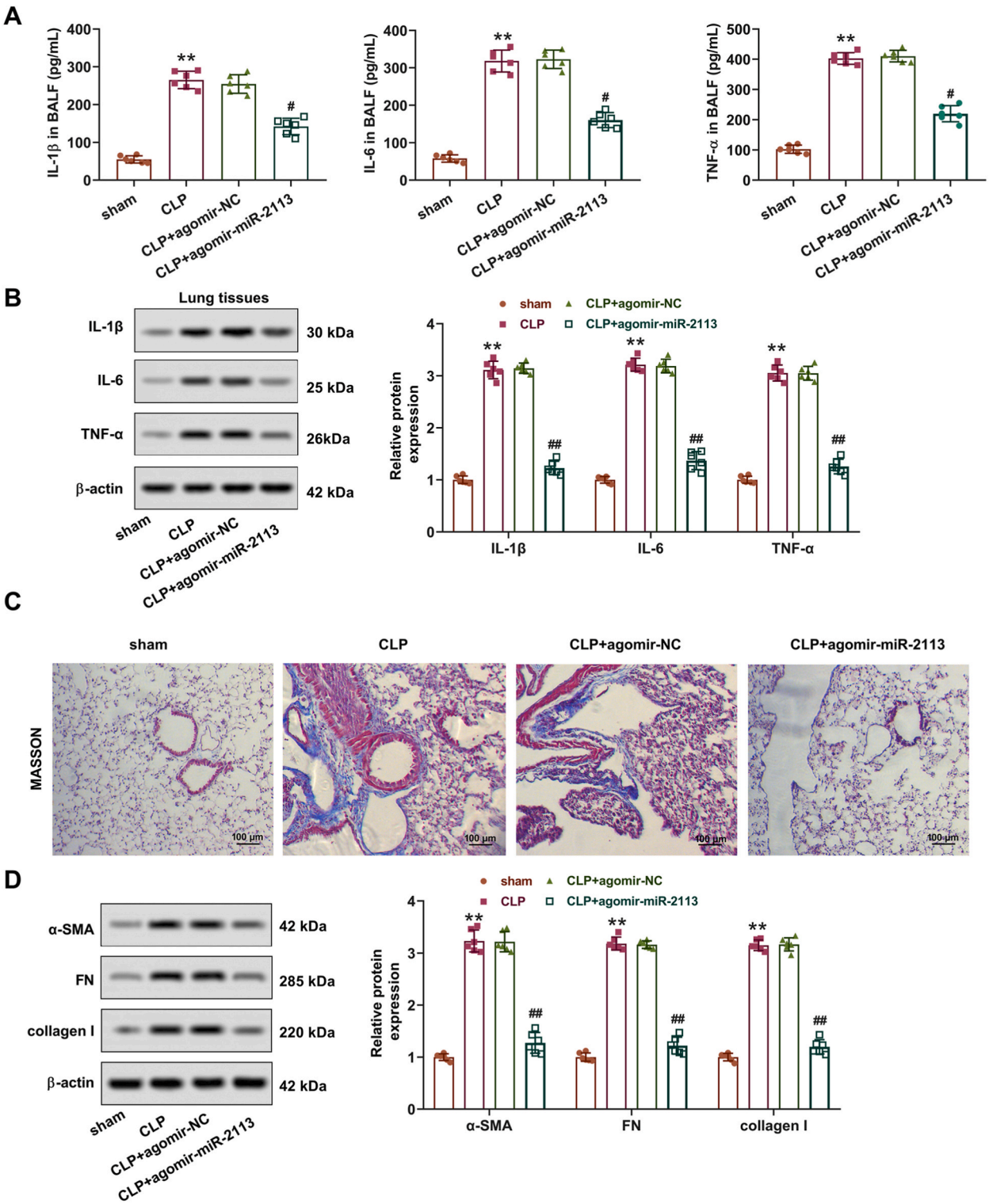

Fig. 6. Influence of miR-2113 on inflammatory and fibrosis markers in sepsis induced-mice. Mice were divided into the sham, CLP, CLP + agomir-NC and CLP + agomir-miR-2113 groups (n = 6 per group). (A) Levels of IL-1β, IL-6, and TNF-α in mouse BALF were checked using ELISA. (B) The protein levels of IL-1β, IL-6, and TNF-α were detected using Western blot. (C) Fibrosis degree of mouse lung tissues was examined by Masson staining (scale bar: 100 μm). (D) The protein levels of α-SMA, FN, and collagen I were examined by Western blot. $^{**}P < 0.01$ vs. sham. $^{\#}P < 0.05$, $^{\#\#}P < 0.01$ vs. CLP + agomir-NC. Differences were assessed with one-way ANOVA followed by Tukey's post-test.

miR-2113 mimic (Fig. 3C, Supplementary File-2). Then, HMGB1 was overexpressed in MLE-12 cells (Fig. 3D, Supplementary File-2). We found that HMGB1 upregulation reduced the proliferation, but increased the apoptosis of MLE-12 cells that were affected by miR-2113 mimic (Fig. 3E–G). Moreover, HMGB1 overexpression promoted the levels of IL-1β, IL-6, and TNF-α that were suppressed by miR-2113 mimic (Fig. 3H). Western blot assay indicated that miR-2113 mimic decreased the protein levels of α-SMA, FN and collagen I, which was abolished by HMGB1 overexpression (Fig. 3I, Supplementary File-2). To sum up, miR-2113 mimic reduced LPS-induced MLE-12 cell injury via negatively regulating HMGB1.

3.4. MiR-2113 overexpression relieves sepsis-induced lung injury in mice

As displayed in Fig. 4A, miR-2113 expression was under-expressed in the lung tissues of CLP mice, while its expression was increased after miR-2113 overexpression. Contrarily, the mRNA and protein levels of HMGB1 were upregulated in the lung samples of CLP mice, whereas miR-2113 agomir decreased its upregulation (Fig. 4B and C, Supplementary File-2). Numerous inflammatory cell infiltration was observed in the alveolar wall and alveolar cavity of CLP mice, but this impact was abolished by agomir-miR-2113 (Fig. 4D). TUNEL analysis revealed that CLP-induced apoptosis of lung tissues was reduced after miR-2113 overexpression (Fig. 4E). In summary, miR-2113 overexpression relieved lung injury in CLP mice.

3.5. MiR-2113 mitigates acute pulmonary dysfunction in mice with CLP-induced sepsis

Subsequently, we elucidated the regulatory role of miR-2113 in acute pulmonary dysfunction induced by sepsis in mice. Our experimental data revealed that airway resistance was increased, and lung ventilation, lung compliance, tidal volume and RR were decreased in CLP mice, while these impacts were reversed after miR-2113 overexpression (Fig. 5A–E). Furthermore, CLP induced the high W/D ratio, which was abolished by agomir-miR-2113 (Fig. 5F). LDH and total protein contents in BALF are also applied to evaluate acute pulmonary dysfunction [20]. As displayed in Fig. 5G and **H**, the LDH and total protein contents in BALF were elevated in CLP mice, which was suppressed by agomir-miR-2113. These findings clarified that miR-2113 overexpression improved acute pulmonary dysfunction in sepsis mice.

3.6. MiR-2113 modulates lung inflammation and fibrosis in sepsis induced-mice

We further verified whether miR-2113 regulated lung inflammation and fibrosis caused by CLP. ELISA data showed that CLP induced high contents of IL-1β, IL-6 and TNF-α in BALF, which was abolished by agomir-miR-2113 (Fig. 6A). Similarly, the protein levels of IL-1β, IL-6 and TNF-α in mouse lung tissues induced by CLP were inhibited by miR-2113 (Fig. 6B, Supplementary File-2). Meanwhile, miR-2113 overexpression abolished CLP-induced fibrosis in mouse lung tissues (Fig. 6C). Additionally, we found that the levels of α-SMA, FN and collagen I were raised by CLP, the effect of which was abolished after miR-2113 overexpression (Fig. 6D, Supplementary File-2). These data indicated that miR-2113 overexpression relieved lung inflammation and fibrosis in sepsis mice.

4. Discussion

Sepsis is recognized as a vital cause of death in critically ill patients [21]. Since ALI is common in severe sepsis [22], this research aimed to elucidate the mechanism of sepsis-induced ALI. Our prominent findings were listed as follows: (I) MiR-2113 expression was lessened in LPS-induced MLE-12 cells and CLP mouse models as well as the serum of sepsis patients. (II) MiR-2113 overexpression promoted proliferation, and alleviated inflammatory and fibrosis markers in LPS-stimulated MLE-12 cells. (III) MiR-2113 mimic relieved LPS-induced MLE-12 cell injury through negatively regulating HMGB1. (IV) MiR-2113 overexpression reduced acute pulmonary dysfunction, inflammation and fibrosis in sepsis-induced mice. These findings suggested that miR-2113 was a novel target for the diagnosis and treatment of sepsis-induced ALI.

Recent findings suggested that abnormal expression of miRNAs might be a key event in the pathogenesis of sepsis-induced ALI. For instance, miRNA-490 relieved sepsis-induced ALI by targeting MRP4 [23]. miR-1224-5p was a factor to promote inflammation and oxidative damage in sepsis-induced ALI [24]. Until now, the miRNAs implicated in sepsis-induced ALI are largely unknown. miR-2113 has been reported to mediate cell proliferation and apoptosis [10,25]. In this research, we supplied compelling evidence supporting the function of miR-2113 in sepsis-induced ALI. *In vitro* studies, miR-2113 was decreased in LPS-induced MLE-12 cells. Transfection of miR-2113 mimic abolished the decrease of proliferation and increase of apoptosis in MLE-12 cells caused by LPS.

Accumulated researches illustrate that the pathogenesis of sepsis-induced ALI is complex and is involved in inflammation. For instance, Wei et al. indicated that IL-5 reduced lung injury by repressing systemic inflammatory response caused by sepsis [26]. Jeong et al. elucidated that Lysophosphatidylcholine alleviated sepsis-induced lung injury by reducing inflammation [27]. Similarly, our experimental data found that miR-2113 overexpression relieved LPS-induced inflammation in MLE-12 cells. Fibrosis is another important inducement of sepsis-induced ALI [28]. Notability, studies have clarified that several miRNAs are associated with sepsis-induced fibrosis, such as miR-130a [29] and miR-122 [30]. Moreover, miR-2113 inhibition restored high glucose-induced mesenchymal cell activation and fibrosis [9]. Our study demonstrated that miR-2113 overexpression reduced LPS-induced fibrosis in MLE-12 cells.

We further elucidated the mechanism of miR-2113 in sepsis-induced ALI. Previous studies demonstrated that miRNAs modulated sepsis-induced ALI process by mediating downstream target genes [31,32]. HMGB1 belongs to high-mobility protein groups and is a common pro-inflammatory factor [33]. Exogenous HMGB1 induced inflammatory responses in tendon cells in a dose-dependent

manner [34], and HMGB1 accelerated epithelial-to-mesenchymal cell transition in crystalline silica-induced pneumonia and fibrosis [35]. Traditional Chinese medicine bupleurum polysaccharides reduced the expressions of collagen I, α-SMA and FN by inhibiting HMGB1 [36]. HMGB1 knockdown suppressed the levels of inflammatory cytokines including IL-6, TNF-α, and IL-1β in endometriosis [37]. Increasing studies indicate that HMGB1 mediates the occurrence of sepsis-induced ALI, and is modulated by diverse miRNAs. For example, Zhou et al. found that miR-126-5p overexpression reduced HMGB1 expression to alleviate LPS-induced lung injury [38]. Yang et al. confirmed that miR-129-5p overexpression alleviated inflammatory responses in sepsis-induced ALI by decreasing HMGB1 [39]. As expected, we also found that miR-2113 mitigated LPS-induced injury of MLE-12 cells by negatively regulating HMGB1. Agomir can be directly dissolved and used in animal experiments compared to mimic according to a previous report [40]. Therefore, miR-2113 agomir and mimic were used to overexpress miR-2113 *in vivo* and *in vitro*, respectively. Our *in vivo* data validated that miR-2113 overexpression ameliorated acute pulmonary dysfunction, inflammation and fibrosis in sepsis mice. The limitations of this research were listed: (I) This research was only implemented through the gain-of-function assay. (2) MiR-2113 might impact sepsis-induced ALI through other mechanisms except for HMGB1. (3) This research only assessed one target gene of miR-2113, and did not explore the signaling pathway. (4) This research did not select human lung cells for functional research.

5. Conclusions

This research demonstrated the low expression of miR-2113 in LPS-induced MLE-12 cells and CLP mouse models as well as the serum of sepsis patients. miR-2113 overexpression attenuated acute pulmonary dysfunction, inflammation and fibrosis in LPS-induced MLE-12 cells and sepsis mice. Furthermore, miR-2113 overexpression relieved LPS-induced MLE-12 cell injury by negatively modulating HMGB1.

Ethics and informed consent

This study was reviewed and approved by the Ethics Committee of The First People's Hospital of Lianyungang, with the approval number: KY-20220226001-02.

All participants/patients provided informed consent to participate in the study.

Data availability statement

Data will be made available on request.

CRediT authorship contribution statement

Yong Li: Formal analysis, Methodology, Writing – original draft. **Hui-Ling Xu:** Data curation, Methodology, Software, Writing – review & editing. **Xiu-Wen Kang:** Data curation, Methodology, Software, Writing – review & editing. **Suo Xu:** Data curation, Software, Writing – review & editing. **Zhi-Fang Mou:** Conceptualization, Project administration, Writing – review & editing.

Declaration of competing interest

The authors declare that they have no known competing financial interests or personal relationships that could have appeared to influence the work reported in this paper.

Acknowledgments

NA.

Abbreviations

Acute kidney injury (AKI)
cecal ligation and puncture (CLP)
microRNAs (miRNAs)
messenger RNAs (mRNAs)
lipolyaccharide (LPS)
bronchoalveolar lavage fluid (BALF)
quantitative real-time PCR (qRT-PCR)
Cell Counting Kit-8 (CCK-8)
enzyme-linked immunosorbent assay (ELISA)
wild-type (WT)
mutant (MUT)
terminal deoxynucleotidyl transferase-mediated dUTP-biotin nick end labeling (TUNEL)
respiratory rate (RR)

Wet/dry (W/D)
lactate dehydrogenase (LDH)
high-mobility group box 1 (HMGB 1)

Appendix A. Supplementary data

Supplementary data to this article can be found online at https://doi.org/10.1016/j.heliyon.2023.e22772.

References

[1] D. Liu, et al., Sepsis-induced immunosuppression: mechanisms, diagnosis and current treatment options, Mil Med Res 9 (1) (2022) 56.
[2] M. Singer, et al., The third international consensus definitions for sepsis and septic shock (Sepsis-3), JAMA 315 (8) (2016) 801–810.
[3] V. Kumar, Pulmonary innate immune response determines the outcome of inflammation during pneumonia and sepsis-associated acute lung injury, Front. Immunol. 11 (2020) 1722.
[4] J.P. Margaria, et al., PI3K signaling in mechanisms and treatments of pulmonary fibrosis following sepsis and acute lung injury, Biomedicines 10 (4) (2022).
[5] C. Wu, et al., Lymphatic flow: a potential target in sepsis-associated acute lung injury, J. Inflamm. Res. 13 (2020) 961–968.
[6] M. Correia de Sousa, et al., Deciphering miRNAs' action through miRNA editing, Int. J. Mol. Sci. 20 (24) (2019).
[7] Z. Wang, et al., MicroRNA-326 prevents sepsis-induced acute lung injury via targeting TLR4, Free Radic. Res. 54 (6) (2020) 408–418.
[8] X. Cao, et al., *MiR-145 negatively regulates TGFBR2 signaling responsible for sepsis-induced acute lung injury.* Biomed Pharmacother 111 (2019) 852–858.
[9] L.P. Xue, et al., Rg1 inhibits high glucose-induced mesenchymal activation and fibrosis via regulating miR-2113/RP11-982M15.8/Zeb1 pathway, Biochem. Biophys. Res. Commun. 501 (4) (2018) 827–832.
[10] L. Zhang, et al., Eukaryotic initiation Factor 4AIII facilitates hepatocellular carcinoma cell proliferation, migration, and epithelial-mesenchymal transition process via antagonistically binding to WD repeat domain 66 with miRNA-2113, J. Cell. Physiol. 235 (11) (2020) 8199–8209.
[11] J. Li, et al., Panaxydol attenuates ferroptosis against LPS-induced acute lung injury in mice by Keap1-Nrf2/HO-1 pathway, J. Transl. Med. 19 (1) (2021) 96.
[12] A. Sang, et al., Quercetin attenuates sepsis-induced acute lung injury via suppressing oxidative stress-mediated ER stress through activation of SIRT1/AMPK pathways, Cell. Signal. 96 (2022) 110363.
[13] D. Liang, et al., Down-regulation of Xist and Mir-7a-5p improves LPS-induced myocardial injury, Int. J. Med. Sci. 17 (16) (2020) 2570–2577.
[14] J. Pan, et al., microRNA-193-3p attenuates myocardial injury of mice with sepsis via STAT3/HMGB1 axis, J. Transl. Med. 19 (1) (2021) 386.
[15] H. Cai, et al., LncRNA AIRN influences the proliferation and apoptosis of hepatocellular carcinoma cells by regulating STAT1 ubiquitination, Arch Pharm. Res. (Seoul) 44 (4) (2021) 414–426.
[16] H.H. Yang, et al., A COX-2/sEH dual inhibitor PTUPB alleviates lipopolysaccharide-induced acute lung injury in mice by inhibiting NLRP3 inflammasome activation, Theranostics 10 (11) (2020) 4749–4761.
[17] N. Takeichi, H. Yamazaki, K. Fujimoto, Comparison of impedance measured by the forced oscillation technique and pulmonary functions, including static lung compliance, in obstructive and interstitial lung disease, Int J Chron Obstruct Pulmon Dis 14 (2019) 1109–1118.
[18] K. Vaporidi, et al., Pulmonary microRNA profiling in a mouse model of ventilator-induced lung injury, Am. J. Physiol. Lung Cell Mol. Physiol. 303 (3) (2012). L199-207.
[19] C. Wang, et al., MicroRNA-762 modulates lipopolysaccharide-induced acute lung injury via SIRT7, Immunol. Invest. 51 (5) (2022) 1407–1422.
[20] Y. Mo, et al., miR-21 mediates nickel nanoparticle-induced pulmonary injury and fibrosis, Nanotoxicology 14 (9) (2020) 1175–1197.
[21] J. Ma, et al., Altered expression of TIAM1 in endotoxin-challenged airway epithelial cells and rodent septic models, J. Thorac. Dis. 10 (6) (2018) 3187–3195.
[22] C. Jin, et al., Gut-lymph-lung pathway mediates sepsis-induced acute lung injury, Chin Med J (Engl) 133 (18) (2020) 2212–2218.
[23] J. Lin, Z. Lin, L. Lin, MiR-490 alleviates sepsis-induced acute lung injury by targeting MRP4 in new-born mice, Acta Biochim. Pol. 68 (2) (2021) 151–158.
[24] B. Liu, et al., MicroRNA-1224-5p aggravates sepsis-related acute lung injury in mice. Oxid med cell longev 2022 (2022) 9493710.
[25] D. Liang, C. Tian, X. Zhang, lncRNA MNX1-AS1 promotes prostate cancer progression through regulating miR-2113/MDM2 axis, Mol. Med. Rep. 26 (1) (2022).
[26] B. Wei, et al., Interleukin IL-5 alleviates sepsis-induced acute lung injury by regulating the immune response in rats, Bioengineered 12 (1) (2021) 2132–2139.
[27] S. Jeong, et al., Lysophosphatidylcholine alleviates acute lung injury by regulating neutrophil motility and neutrophil extracellular trap formation, Front. Cell Dev. Biol. 10 (2022) 941914.
[28] J. Villar, et al., Early activation of pro-fibrotic WNT5A in sepsis-induced acute lung injury, Crit. Care 18 (5) (2014) 568.
[29] J. Ding, et al., DNMT1/miR-130a/ZEB1 regulatory pathway affects the inflammatory response in lipopolysaccharide-induced sepsis, DNA Cell Biol. 41 (5) (2022) 479–486.
[30] C. Roderburg, et al., Elevated miR-122 serum levels are an independent marker of liver injury in inflammatory diseases, Liver Int. 35 (4) (2015) 1172–1184.
[31] K. Shen, et al., miR-125b-5p in adipose derived stem cells exosome alleviates pulmonary microvascular endothelial cells ferroptosis via Keap1/Nrf2/GPX4 in sepsis lung injury, Redox Biol. 62 (2023) 102655.
[32] Q. Lu, et al., miR-942-5p prevents sepsis-induced acute lung injury via targeting TRIM37, Int. J. Exp. Pathol. 102 (4–5) (2021) 192–199.
[33] Z. Rao, et al., Corrigendum: 1,25-dihydroxyvitamin D inhibits LPS-induced high-mobility group box 1 (HMGB1) secretion via targeting the NF-E2-Related factor 2-hemeoxygenase-1-HMGB1 pathway in macrophages, Front. Immunol. 9 (2018) 357.
[34] C. Zhang, et al., Extracellular HMGB-1 activates inflammatory signaling in tendon cells and tissues, Ther Adv Chronic Dis 11 (2020), 2040622320956429.
[35] J. Ma, et al., High-mobility group box 1 promotes epithelial-to-mesenchymal transition in crystalline silica induced pulmonary inflammation and fibrosis, Toxicol. Lett. 330 (2020) 134–143.
[36] Z.Z. Liu, et al., Bupleurum polysaccharides ameliorated renal injury in diabetic mice associated with suppression of HMGB1-TLR4 signaling, Chin. J. Nat. Med. 17 (9) (2019) 641–649.
[37] J. Huang, X. Chen, Y. Lv, HMGB1 mediated inflammation and autophagy contribute to endometriosis, Front. Endocrinol. 12 (2021) 616696.
[38] Y. Zhou, et al., Exosomes from endothelial progenitor cells improve outcomes of the lipopolysaccharide-induced acute lung injury, Crit. Care 23 (1) (2019) 44.
[39] P. Yang, et al., Overexpression of miR-129-5p Mitigates Sepsis-Induced Acute Lung Injury by Targeting High Mobility Group Box 1, J Surg Res 256 (2020) 23–30.
[40] H. Ren, W. Mu, Q. Xu, *miR-19a-3p inhibition alleviates sepsis-induced lung injury via enhancing USP13 expression.* Acta Biochim Pol 68 (2) (2021) 201–206.